Electronic Supplementary Material (ESI) for RSC Advances.

Hierarchical Metal Nanomesh/Microgrid Structures for High Performance Transparent Electrodes

Tongchuan Gao, Po-shun Huang, Jung-kun Lee, and Paul W. Leu*

Department of Industrial Engineering and Department of Mechanical Engineering and Materials Science, University of Pittsburgh, Pittsburgh, Pennsylvania, USA

E-mail: pleu@pitt.edu

Simulations

The transmission and sheet resistance of metal NMs and MGs were investigated separately. For metal NMs, the finite difference time domain (FDTD) method[1,2] was used to solve Maxwell's equations and simulate the optical transmittance. The refractive index for Ag was taken from *CRC Handbook of Chemistry and Physics*.[3] Perfectly matched layer (PML) boundary conditions were used for the upper and lower boundary of the simulation cell,[4] while periodic boundary conditions with appropriate symmetries were used for the side boundaries to model the interaction between the periodic structure and the polarized incident light. A non-uniform mesh was utilized so that the mesh is finer near the interfaces between Ag NM and environment and larger in the bulk regions of Ag NM and environment to improve the simulation accuracy and reduce the memory requirement.

*To whom correspondence should be addressed

Ag NMs constitute diffraction gratings where diffraction occurs when $\vec{k}_{(pq)} = \vec{k}_{in} + p\vec{b_1} + q\vec{b_2}$ holds, where $\vec{k}_{(pq)}$ is the wave vector of the diffraction spot, $\vec{k}_{in}$ is the wave vector of the incident light, $\vec{b_1}$ and $\vec{b_2}$ are the reciprocal lattice basis, and p and q are integers. The transmitted power scattered into a particular grating order was determined based on the far field projection of the transmission. The specular transmission was determined from the $(0, 0)$ order transmission, and the diffusive transmission was determined from the total power of all light transmitted through all diffraction orders. The transmission is anisotropic, but invariant under 60° rotational transformations. We utilized angle averaged transmission $T_{NM} = \frac{1}{2}(T_{NM,xx} + T_{NM,yy})$ for comparison between different geometries, where T_{xx} and T_{yy} are the transmission for light polarized in the x- and y-directions respectively, as shown in Figure 1a in the article.

For the Ag MG, the transmission was assumed for simplicity to be the geometrical opening $T_{MG} = [(a_{MG} - w_{MG})/a_{MG}]^2$, which is independent upon incident wavelength. The transmission of the hierarchical structure is calculated from $T = T_{NM} \cdot T_{MG}$. The optical interaction between the two layers were neglected, because the dimensions of the metal MG are much greater than the incident wavelength and the NM layer underneath.

To determine the sheet resistances of Ag NM and MG, we used the finite element method (FEM) to solve Poisson's and current continuity equations. The sheet resistance for Ag NM, $R_{s,NM}$, and Ag MG, $R_{s,MG}$, were simulated respectively. The simulations assumed the Ag resistivity in the structure is the bulk resistivity ($\rho_{Ag} = 1.59 \times 10^{-8}$ Ω·m).[3] A rectangular supercell was modeled for Ag NM and MG with electric potential V_a imposed on one of the side boundaries and ground on the opposite boundary. To simulate the infinite periodic structure, zero normal current density boundary condition was used on the other two side boundaries. Insulation boundaries were used at any other surfaces of NM and MG. The electric current was obtained by simulation and thus the sheet resistance was calculated. We obtained the normal current I_{norm} by integrating the current density J_{norm} over the ground side and the sheet resistance R_s was calculated from $R = \frac{V_a}{I_{norm}} = R_s \frac{L}{W}$ where L and W

are the length and width of the simulation cell. The Ag NM and MG both possess a six-fold symmetry and our simulations indicated very little dependence of sheet resistance on transport direction. We utilized $R_s = \frac{1}{2}(R_{s,xx} + R_{s,yy})$, where $R_{s,xx}$ and $R_{s,yy}$ are the sheet resistances in the x- and y-direction for either NMs or MGs, where one of the two directions is in the direction of one of the two lattice vectors. The Ag NM and MG are treated as connected in parallel, thus the sheet resistance R_s is calculated from $1/R_s = 1/R_{s,NM} + 1/R_{s,MG}$.

Design Criterion for Ag NM/MG

For the Ag MG, the criterion of $T > 90\%$ at $R_s < 10$ Ω/sq is satisfied with four different designs. The masks for photolithography have the following geometric parameters: (1) $a = 200$ μm, $w = 5$ μm; (2) $a = 300$ μm, $w = 10$ μm; (3) $a = 500$ μm, $w = 5$ μm; and (4) $a = 500$ μm, $w = 10$ μm.

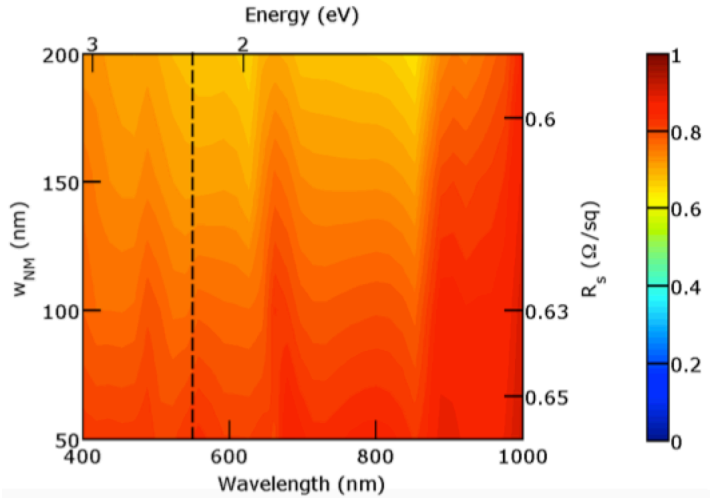

Figure S1: Contour plot of angle averaged transmission for various w_{NM} with $a_{NM} = 2000$ nm, $t_{NM} = 30$ nm, $a_{grid} = 200$ μm, width $w_{grid} = 5$ μm, and $t_{grid} = 1$ μm as a function of wavelength. The calculated sheet resistance, which depends on w_{NM}, is shown on the right axis of the plot. The dashed black line indicates $\lambda = 550$ nm, which was used in the previous Figure.

Figure S1 shows a contour plot of the optical transmission for Ag NM/MG as a function of w_{NM} between 50 and 200 nm and wavelength between 400 nm and 1000 nm. The pitch for Ag NM is $a_{NM} = 2000$ nm and the thickness is $t_{NM} = 30$ nm. The pitch for the Ag MG is

$a_{MG} = 200$ μm, the width is $w_{MG} = 5$ μm, and the thickness is $t_{MG} = 1$ μm. The simulated angle averaged sheet resistances are shown on the right y-axis. The angle averaged sheet resistances range from $R_s = 0.59$ Ω/sq for $w_{NM} = 200$ nm to $R_s = 0.66$ Ω/sq for $w_{NM} = 50$ nm. While other work has demonstrated extraordinary transmission for sub-wavelength holes at particular wavelengths due to surface plasmon modes[5] and propagating plasmonic modes,[6] the NMs in this work contain apertures with sizes greater than the wavelengths of interest, such that there is broadband transmission close to unity. The peaks and dips in the transmission spectra is primarily due to the excitation of propagating modes in the NM holes. Cylindrical holes in a perfect metal support propagating modes at wavelengths $\lambda \lesssim 2d$,[5] which covers the entire spectrum studied, since the smallest hole diameter studied was $d = 1800$ nm where $w_{NM} = 200$ nm. For Ag NM/MG, a broadband transmission over 80% is achievable for $R_s \leq 1$ Ω/sq. In addition, surface waves are resonantly excited by the NMs when $\vec{k}_{spp}(\lambda_{mn}) = \vec{k}_{in,x} + m\vec{b_1} + n\vec{b_2}$ where $\vec{k}_{spp} = \frac{2\pi}{\lambda}\sqrt{\frac{\epsilon}{\epsilon+1}}$ is the wave vector of the surface plasmon polariton, $\vec{k}_{in,x}$ is the in-plane component of the incident wave vector, ϵ is the permittivity of the Ag, and m and n are integers. The reciprocal lattice basis vectors are $\vec{b}_1 = \left(\frac{2\pi}{a}, -\frac{2\sqrt{3}\pi}{3a}\right)$ and $\vec{b}_2 = \left(0, \frac{4\sqrt{3}\pi}{3a}\right)$. For normal incidence light, surface plasmon polaritons are excited when $|\vec{k}_{spp}(\lambda_{mn})| = \frac{2\pi}{a}\sqrt{\frac{4}{3}(m^2 + n^2 - mn)}$, corresponding to the Fano type features.[7] For example, the Fano type feature at $\lambda = 1000$ nm corresponds to the $(2, 1)$, $(1, 2)$, $(-1, 1)$, or $(1, -1)$ surface plasmon polariton.

Ag MG Fabrication

Ag MG was fabricated using lift-off metal patterning. For a smoother metal profile and a better lift-off result, the bilayer method was used. A layer of MicroChem LOR 5B resist was coated onto a 0.5 mm thick quartz substrate by spin-coating. Then the sample was soft-baked on a hot-plate for 5 minutes at 150 °C. Then a 2 μm thick photoresist AZ 4210 from AZ was spin-coated onto the sample, followed by a soft-bake at 120 °C for 2 minutes. The photoresist was exposed using $\lambda = 365$ nm (i-line) light and then developed in diluted

AZ 400 K from AZ for 15 seconds, which allowed undercut of the LOR 5B layer to form a photoresist profile favorable for lift-off. A thin layer of titanium was first deposited as an adhesion layer onto the patterned photoresist with an e-beam evaporator, followed by Ag deposition. Then, the photoresist was removed using Shipley 1165 developer remover at room temperature with gentle ultrasonication.

References

(1) Yee, K. *Antennas and Propagation, IEEE Transactions on* **1966**, *14*, 302–307.

(2) Taflove, A. *Electromagnetic Compatibility, IEEE Transactions on* **1980**, *EMC-22*, 191–202.

(3) Lide, D. *2010, CRC handbook of chemistry and physics*; CRC Press/Taylor and Francis, 2010.

(4) Berenger, J. *Journal of Computational Physics* **1994**, *114*, 185–200.

(5) Ebbesen, T. W.; Lezec, H. J.; Ghaemi, H. F.; Thio, T.; Wolff, P. A. *Nature* **1998**, *391*, 667–669.

(6) Shin, H.; Catrysse, P. B.; Fan, S. *Physical Review B* **2005**, *72*, 085436.

(7) Fano, U. *Physical Review* **1961**, *124*, 1866–1878.